



Cite this: *J. Mater. Chem. C*, 2016, 4, 6287

## ON/OFF switching of silicon wafer electrochemistry by pH-responsive polymer brushes†

G. Panzarasa,‡§\*<sup>a</sup> M. Dübner,‡<sup>bc</sup> V. Pifferi,‡\*<sup>de</sup> G. Soliveri,¶<sup>d</sup> and C. Padeste<sup>c</sup>

pH-Switchable electrochemical properties are demonstrated for the first time for native oxide-coated silicon wafer electrodes. Ultrathin and ultrathick pH-responsive poly(methacrylic acid) (PMAA) brushes, obtained by surface-initiated atom transfer radical polymerization, were used to achieve redox gating. PMAA brushes are reversibly switched between their protonated and deprotonated states by alternating acidic and basic pH, which corresponds to a swelling/collapsing behavior. As a result, the electrochemical properties of the PMAA brush-modified silicon electrode are switched "ON" and "OFF" simply by changing pH. The electrochemical properties of the modified electrode were examined by means of cyclic voltammetry and electrochemical impedance spectroscopy both in the absence and presence of ruthenium(III) hexamine, a well-known cationic redox probe.

Received 4th May 2016,  
Accepted 1st June 2016

DOI: 10.1039/c6tc01822j

www.rsc.org/MaterialsC

### Introduction

Computer science as we know it would not exist without Boolean logic and logic gates. In principle, even the smartest electronic gadget – be it a smartphone, a laptop or a tablet – owes its performances to a few simple components which process one or more logical inputs producing a single logical output, either true (one, on) or false (zero, off). Logic gates are essential elements making up digital circuits in computer chips, including the simplest of them, the ON/OFF switch.

The fabrication of logic gates is by no means limited to the realm of solid state physics: logic gates operated by supramolecular assemblies,<sup>1–3</sup> nanoparticles,<sup>4,5</sup> enzymes<sup>6–8</sup> and DNA strands<sup>9</sup> have been described.

Nowadays, stimuli-responsive polymer brushes represent the most promising frontier in this field.<sup>10</sup> Polymer brushes

are ultrathin polymer layers in which the polymer chains are tethered at one end to a surface. They are usually formed in a polymerization reaction in which chain growth is started directly from a suitable initiator-functionalized substrate. Polymer brushes are a hot topic in modern surface and polymer science thanks to their unique properties, such as high versatility and high density of functionalities.<sup>11–14</sup> They enable the development of functional interfaces with switchable properties controlled by external physical (*e.g.* heat,<sup>15</sup> light,<sup>16</sup> electricity,<sup>17</sup> and magnetism<sup>18</sup>) or chemical (*e.g.* the presence or absence of chemicals, variation of their concentrations) inputs and have therefore received considerable attention in the last two decades.<sup>19</sup>

The use of polymer brushes as an alternative approach to direct the fabrication of molecular electronics and devices is highly appealing: poly(methyl methacrylate) (PMMA) and poly(styrene) (PS) brushes have been described to perform as electrets<sup>20</sup> or as gate dielectrics in all-organic transistors.<sup>21–23</sup>

Polymer brushes modified with electroactive units, such as ferrocene,<sup>24</sup> osmium complexes,<sup>25</sup> carbazole<sup>26</sup> and nitroxide<sup>27</sup> pendants have been studied. Recently, an elegant approach to transform polymer brushes into conjugated poly(acetylene)-like "molecular wires" was described.<sup>28</sup> Despite these encouraging results, however, there is still much room for improvement especially for electrochemical applications.<sup>29</sup>

Polyelectrolyte brushes, *i.e.* polymer brushes carrying acidic, basic or ionic groups in their repeat units, represent a simpler and more convenient approach for the development of electrochemical logic gates, due to their high sensitivity to pH and to different ionic species.<sup>30,31</sup> Such gates are circuit logic elements which, in contrast to conventional solid-state devices, operate and receive their inputs being immersed in

<sup>a</sup> Dipartimento di Scienze e Innovazione Tecnologica, Università del Piemonte Orientale "Amedeo Avogadro", Viale T. Michel 11, 15100 Alessandria, Italy. E-mail: gp4779@gmail.com

<sup>b</sup> Laboratory for Surface Science and Technology, Department of Materials, ETH Zürich, CH-8093 Zürich, Switzerland

<sup>c</sup> Laboratory for Micro- and Nanotechnology, Paul Scherrer Institute, CH-5232 Villigen PSI, Switzerland

<sup>d</sup> Dipartimento di Chimica, Università degli Studi di Milano, Via Golgi 19, 20133 Milano, Italy. E-mail: valentina.pifferi@unimi.it

<sup>e</sup> Consorzio Interuniversitario per la Scienza e Tecnologia dei Materiali (INSTM), Via Giusti 9, 50121 Firenze, Italy

† Electronic supplementary information (ESI) available: Additional data and figures. See DOI: 10.1039/c6tc01822j

‡ These authors contributed equally.

§ Present address: Empa Materials Science and Technology, Lerchenfeldstrasse 5, 9014 St. Gallen, Switzerland.

¶ Department of Engineering Physics, Polytechnique Montréal Succ. Centre-ville, 6079 Montréal, Quebec, H3C 3A7 Canada.



electrolyte solutions.<sup>32</sup> Modifying the electrode surface with responsive polymer brushes offer the possibility of directly switching their charge-transfer properties ON/OFF upon the application of an external stimulus, such as temperature, ionic force or pH. Recent literature featured the development of electrochemical biosensors and computing devices in which pH-responsive polymer brushes acted as a redox gate layer.<sup>33–37</sup>

It is important now to state that all the previously cited studies have been performed on brush-modified conventional, *i.e.* highly conductive, electrodes such as gold and fluoride- or indium-doped tin oxide (FTO, ITO). Silicon wafers, being the workhorse substrate of microelectronics, would provide a more affordable, versatile and easily scalable scaffold for the development of electrochemically active polymer–Si hybrids. However, the lack of affinity towards conventional redox probes and its nm-thick native oxide layer acting as a barrier toward electron transfer make silicon a very poor electrode material.<sup>38</sup>

In a recent paper<sup>29</sup> we demonstrated how these problems can be overcome by the grafting of polymer brushes. We studied hydrophilic and cationic brushes made of both homo- and copolymers of 2-hydroxyethyl methacrylate (HEMA) and 2-aminoethyl methacrylate (AMA), which were grown on native oxide-coated silicon wafers. Using electrochemical impedance spectroscopy (EIS) we showed that even poly(HEMA) brushes were able to make silicon wafers responsive to ferrocyanide, a common redox probe. Considering the opportunities offered by polymer brushes for surface engineering, it is apparent that these results open the path to design a new class of electrochemical devices *e.g.* for sensing applications. To further explore the possibilities offered by polymer brushes for the development of innovative silicon-based electrochemical devices, we turned our attention to anionic polyelectrolytes. Poly(methacrylic acid) (PMAA) was selected because of its well-known reversible pH-responsive behavior, which could be useful for advanced microfluidic and lab-on-chip devices. Furthermore, controlled polymerization protocols such as atom transfer radical polymerization (ATRP) are well established for monomers such as methacrylic acid.<sup>39</sup>

Here we studied the electrochemical performances of grafted-from ultrathin (14 nm-thick) and ultrathick (1  $\mu\text{m}$ -thick) PMAA brushes grown on native oxide-coated silicon. We found that PMAA brushes, compared to previously investigated polymers, are significantly more efficient to implement electrochemical responsiveness in silicon wafer substrates: the redox reaction of the probe at the modified electrode was clearly demonstrated not only by applying sophisticated techniques such as EIS but also by cyclic voltammetry (CV). Moreover, this response can be reversibly switched ON and OFF simply by changing the pH.

## Experimental

### Materials and methods

All chemicals were of reagent or analytical purity grade, were purchased from Aldrich and used as received. Methacrylic acid

(MAA) was used as received. The (3-(2-bromoisobutyramido)-propyl)triethoxysilane (BIB-APTES) initiator was synthesized and grafted on the surface of piranha-cleaned silicon wafer using an optimized procedure, described in our previous studies.<sup>12–14,29</sup> Water obtained from a Millipore MilliQ water purification system (resistivity  $\geq 18.2 \text{ M}\Omega \text{ cm}^{-1}$ ) was thoroughly used. Silicon(100) wafers, double-polished, n-type, phosphorus-doped, 3–6  $\Omega \text{ cm}$ , were purchased from Ultrasil Corporation.

Brush film thickness was determined by variable angle spectroscopic ellipsometry (VASE) (M-2000F, LOT Oriel GmbH, Darmstadt, Germany), in air, water, HCl and NaOH solutions using a custom-built liquid cell. Determination of  $\Psi$  and  $\Delta$  as a function of wavelength (250–800 nm) was carried out by employing the WVASE32 software package (LOT Oriel GmbH, Darmstadt, Germany), using bulk dielectric functions for silicon, silicon dioxide and water. The brush-supporting substrates were in all cases considered as consisting of silicon with a 2 nm-thick silicon dioxide film. The analysis of the brush layers was performed using a Cauchy model:  $n = A + B/\lambda - 2$ . For dry measurements, the ambient was air, for which a refractive index  $n = 1$  was taken. The film thickness ( $T$ ) and the two Cauchy parameters  $A$  and  $B$  were set as fitting parameters. For measuring the thickness of films in aqueous solutions, the swollen PMAA layer was fitted by a two-component effective medium approximation (EMA) model (Si/SiO<sub>2</sub>/EMA-PMAA/water-ambient) in which the refractive index of water was taken from the Palik handbook. In this case,  $T$  and water content ( $w$ ) of the PMAA layer were set as fitting parameters. Prior to the measurements in solution, the brush samples were allowed to swell for 1 h.

The morphology of polymer brushes was analyzed by atomic force microscopy (AFM), using ScanAssistMode™ on a Dimension Icon instrument with ScanAssistAir™ silicon nitride (Si<sub>3</sub>N<sub>4</sub>) cantilevers with a tip radius of 12 nm, a spring constant of 0.4 N m<sup>-1</sup> and a resonance frequency of 70 kHz.

Water contact angle measurements were performed using DataPhysics OCA 25 and evaluated using SCA 20 software.

Electrochemical measurements were performed using a potentiostat/galvanostat Autolab PGSTAT204 (Metrohm, The Netherlands) equipped with a FRA module. A standard three-electrode cell with a saturated calomel, a Pt wire and a modified silicon wafer as reference, counter- and working electrodes, respectively, was employed. Aqueous 0.1 M KCl (pH 7) was used as the supporting electrolyte. Cyclic voltammetry (CV) was performed by scanning the potential between  $-0.75 \text{ V}$  and  $+0.4 \text{ V}$  (SCE) (scan rate  $0.1 \text{ V s}^{-1}$ ). Electrochemical impedance spectroscopy (EIS) was carried out at  $-0.25 \text{ V}$ ,  $+0.15 \text{ V}$  and  $+0.25 \text{ V}$  (SCE) in the presence or in the absence of 3 mM [Ru(NH<sub>3</sub>)<sub>6</sub>]Cl<sub>3</sub> as a redox probe. Impedance data were fitted by using ZView 2.0 software. The brush samples were allowed to equilibrate with the electrolyte solution for 5–10 min. This timescale proved to be more than adequate as no noticeable change in the electrochemical results was observed for longer times (see Fig. S3, ESI†). The samples were cleaned with copious amounts of deionized water before and after each set of measurements and dried under a nitrogen stream. To study the effect of pH on the electrochemical properties of the brush-modified electrodes,



the samples were immersed in dilute aqueous HCl or NaOH solutions at the desired pH for 15 min, rinsed with water and immersed in the supporting electrolyte to perform the electrochemical measurements.

### Grafting-from of poly(methacrylic) acid (PMAA) brushes

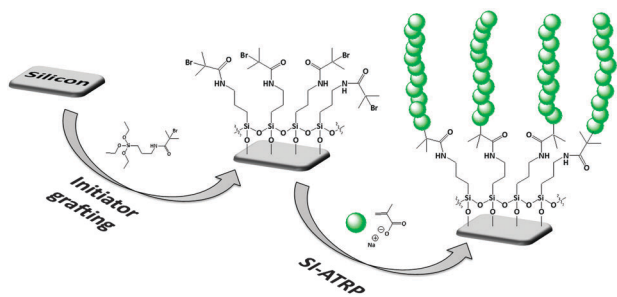
For the grafting-from of ultrathin (14 nm) PMAA brushes, first a solution obtained by dissolving NaOH (4 g, 0.1 mol) in water (15 mL) was cooled in an ice bath. Then, methacrylic acid (MAA, 8.5 mL, 0.1 mol) was added dropwise under stirring to reach a pH  $\sim$  7. The resulting solution was then completely degassed by bubbling nitrogen. Meanwhile, bipyridyl (0.8 g, 5.1 mmol) and CuBr (0.29 g, 2 mmol) were mixed in a Schlenk flask under nitrogen and dissolved in 10 mL of previously degassed methanol. The NaMAA solution was then added under stirring, under a blanket of nitrogen, to the copper complex solution. The resulting polymerization mixture was poured over the initiator-functionalized substrates, placed separately in nitrogen-purged Schlenk flasks, and the polymerization was allowed to proceed for 2 h at 30 °C. After polymerization the samples were washed and gently sonicated with water and eventually dried under a nitrogen stream.

To obtain ultrathick (1  $\mu$ m) PMAA brushes almost the same procedure described for the synthesis of thin brushes was followed. However, after the complete addition of MAA the pH was adjusted to 9 using a concentrated aqueous solution of NaOH.

## Results and discussion

### Grafting-from of PMAA brushes and their pH-responsive behavior

Several procedures are available for the synthesis of polymer brushes on surfaces using the grafting-from approach. Among these, surface-initiated atom-transfer radical polymerization (SI-ATRP) is especially attractive thanks to its tolerance to water, its compatibility with a wide range of functional monomers and the possibility of polymerization at ambient temperature. In the present work, we performed the synthesis of both 14 nm- and 1  $\mu$ m-thick PMAA brushes using a conventional SI-ATRP approach (Scheme 1). Such a dramatic difference in thickness was obtained by changing the pH of the polymerization mixture (see the Experimental section).



Scheme 1 Steps required for the grafting-from of PMAA brushes on silicon wafer.

We focused our attention on ultrathin brushes, because 10–20 nm have been reported as the most suitable thicknesses for applications in organic electronics,<sup>40</sup> allowing scale-down of devices to submicron sizes. As shown by AFM measurements (Fig. S1, ESI<sup>†</sup>), the obtained brushes were homogenous and smooth (average surface roughness  $R_a \leq 1$  nm). Based on ellipsometric measurements and assuming a surface grafting density of 0.4 chains  $\text{nm}^{-2}$  we calculated average molecular weights of  $2.3 \times 10^4$  and  $1.7 \times 10^6$   $\text{g mol}^{-1}$  for the ultrathin and ultrathick brushes, respectively (ESI,† page S2).

The pH-responsive properties of the PMAA brushes could be easily deduced, both from the change in the water contact angle (ranging from  $\sim 40^\circ$  at pH 2 to  $\sim 9^\circ$  at pH 13) as well as from a significant swelling of the brushes exposed to pH  $\gg$   $\text{p}K_a$ . By using AFM and ellipsometric measurements, it was already demonstrated in the literature that the thickness of a PMAA brush can increase up to  $\sim 300\%$  when the pH is switched from 3 to 10.<sup>41</sup> In the present work, spectroscopic ellipsometry was employed to measure the changes in the brush thickness as a function of distinct pH values (Table S1, ESI<sup>†</sup>). In accordance with previous findings, a swelling of more than 400% was observed for our PMAA brushes exposed to a pH 13 solution.

It is known that the behavior of carboxylic group-bearing polymer brushes can be very different from that of the free polymer and the monomer as a result of surface confinement and of Coulombic repulsion of neighboring charges.<sup>42</sup> A dramatic shift in the  $\text{p}K_a$  has been experimentally observed for PMAA brushes (compared to untethered polymer) using FTIR titration,<sup>39</sup> ellipsometric<sup>39,43</sup> and AFM swelling measurements.<sup>41</sup> According to the literature,<sup>39</sup> we expect  $\text{p}K_a \approx 6.5$  for the PMAA brushes.

### Electrochemical and pH-responsive redox gating properties of PMAA brushes on silicon wafer

Cyclic voltammetry (CV) and electrochemical impedance spectroscopy (EIS) were selected to perform a thorough investigation of the properties of the modified silicon electrodes and to what extent those were affected by pH. The ruthenium hexamine  $\text{Ru}(\text{NH}_3)_6^{2+/3+}$  redox couple was chosen as a redox probe to demonstrate the electrochemical properties of PMAA brushes.

**Cyclic voltammetry (CV) of ultrathin polymer brushes.** The cyclic voltammetry plots of ultrathin PMAA brushes performed in the supporting electrolyte (KCl 0.1 M, pH 7) were featureless, showing that PMAA brushes themselves have no electrochemical properties. No significant difference could be observed between the pristine silicon wafer and the PMAA brush-modified silicon wafer. Upon addition of the redox probe ruthenium(III) hexamine to the supporting electrolyte, two defined peaks, attributed to the reduction and oxidation reactions of the redox probe, respectively, readily appeared for the PMAA brush samples. However, unmodified silicon wafers did not show any interaction with this redox probe (Fig. S2, ESI<sup>†</sup>), in complete accordance with our previous findings.<sup>29</sup>

As the methacrylic acid was neutralized with sodium hydroxide before polymerization and a  $\text{p}K_a \approx 6.5$  for the brushes was assumed, it is reasonable to expect that at pH 7 the brushes will contain a sufficient number of negatively charged carboxylate



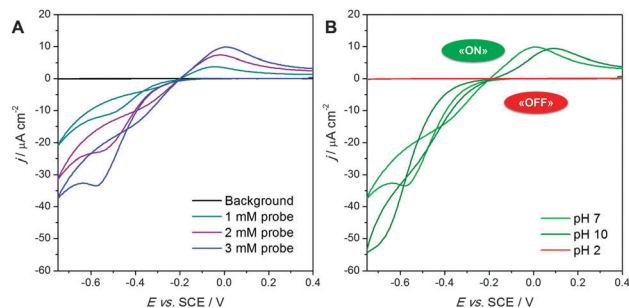


**Fig. 1** (A) Cyclic voltammograms obtained for ultrathin PMAA brushes examined at pH 7 in the absence (background) and presence of increasing concentrations (1 mM, 2 mM and 3 mM) of ruthenium(III) hexamine. (B) Effect of pH on the CV of ultrathin PMAA brushes in the presence of a 3 mM redox probe. The pH values refer to those of the solutions used to condition the brushes before performing the CV. The behavior of PMAA brushes at pH 2 is the same as in the absence of the redox probe: this corresponds to the “OFF” state.

groups, which are very prone to electrostatic interactions with the cationic redox probe. The anionic brushes would thus act as “tentacles”, collecting and concentrating the redox probe molecules and forcing them to be in proximity to the electrode surface where electron transfer can occur (Scheme S1, ESI†).

The intensity of these peaks increased linearly as a function of the redox probe concentration (Fig. 1a). However, the shape of the voltammograms is peculiar, in that the peak-to-peak distance is one order of magnitude higher compared to those obtained with bare or PMAA brush-modified conventional electrodes (see Fig. S3 (ESI†) and Li *et al.*<sup>35</sup>). This finding indicates a less reversible redox behavior.

Such a behavior could be considered anomalous, since the  $\text{Ru}(\text{NH}_3)_6^{2+/3+}$  redox couple usually follows an outer-sphere charge transfer mechanism *i.e.* it is influenced mainly by the density of the electronic states and not by the microstructure of the electrode material. We suggest two possible explanations to account for the observed phenomena. One could be that the electron transfer behavior for the  $\text{Ru}(\text{NH}_3)_6^{2+/3+}$  reaction is changed to an inner-sphere one<sup>42</sup> as a result of electrostatic interaction: the ruthenium hexamine molecules inside the brushes are surrounded by charged carboxylate groups and the resulting polarization could alter the electron transfer dynamics. However, this is not in agreement with literature results,<sup>35</sup> which show that the electrochemical behavior of the ruthenium hexamine probe is not affected by PMAA brushes, at least not for PMAA brushes grafted on conventional (gold) electrodes. The alternative explanation involves the mechanism of electron transfer between the redox probe and our modified silicon electrodes. Due to the presence of an insulating layer of native oxide, electron transfer should occur mainly by tunneling.<sup>44</sup> According to the literature,<sup>45,46</sup> this is possible for a thickness of less than 3 nm. The ellipsometric thickness of the native oxide layer for our electrodes is about 1.5 nm. To allow electron tunneling, the redox probe must be close to the electrode: in our case, this condition would be fulfilled by the pre-concentration effect of the brushes, which capture the redox probe holding it in place. The native oxide layer would

act as a kinetic barrier for electron transport, introducing the observed larger separation between the oxidation and reduction peaks, as already described in the literature for redox-active monolayers on  $\text{SiO}_2$ -coated silicon electrodes.<sup>45</sup>

Fig. 1b shows the effect of pH on the cyclic voltammetry of PMAA brushes in the presence of 3 mM ruthenium(III) hexamine. Experiments at pH 7 were performed directly on as-synthesized brushes, while, to perform the experiments at pH 2 and 10, the brushes were equilibrated in aqueous HCl or NaOH solutions, respectively, for 15 min before performing the CV scans in fresh supporting electrolyte at pH 7. In this way the effects due to ionic force, which otherwise would interfere with the behavior of the redox probe, have been minimized.

After exposure to a pH 2 solution, PMAA brushes showed no electrochemical response in the presence of the redox probe. This demonstrates that pH dramatically changes the interaction between the brushes and the redox probe. It is expected that for a  $\text{pH} \gg \text{pK}_a$  the carboxylic acid groups would be fully protonated, thus deleting the electrostatic affinity for the charged redox probe. Swelling studies performed by ellipsometry at different pH values showed that the PMAA brushes were collapsed at low pH and fully swollen at high pH (Table S1, ESI†). This collapse under acidic conditions would significantly contribute to the reduction in the interaction of the brushes with the electrolyte and thus with the redox probe (see Scheme S1, ESI†).

The electrochemical behavior of PMAA brushes conditioned at pH 10 was comparable to that observed for the brushes at pH 7. However, the redox peaks and especially the reduction one were less reversible at basic pH, probably due to a stronger electrostatic interaction between the fully deprotonated anionic brushes and the cationic probe, stabilizing the electronic structure of the redox probe and penalizing the electrochemical reaction.

Noteworthy, the redox probe inside the brushes could be easily removed by washing the modified electrode with water or fresh electrolyte. This is not surprising, considering the relatively low activation barriers for entry and exit of cationic molecules from a polycarboxylate layer.<sup>47</sup> The absence of a “memory effect” due to irreversible binding of the redox probe could be of great importance for the practical implementation of this system, *e.g.* in microfluidic systems.

**CV of ultrathick PMAA brushes.** The results obtained by cyclic voltammetry for ultrathick PMAA brushes were very similar to those already discussed for the ultrathin ones. The cyclic voltammograms obtained without the redox probe were featureless, while the sequential addition of the redox probe generated the expected two peaks whose intensity increased linearly with the concentration of the added redox probe (Fig. 2a). The peak currents were by a factor of 10 bigger than the ones observed for ultrathin brushes. In addition, much higher capacitive background currents were observed, a direct consequence of increased thickness.

Moreover, compared to the results obtained for ultrathin brushes, the reduction peak was shifted to lower potential values (−450 mV compared to −580 mV in presence of 3 mM redox probe) and much less dependent on the redox probe



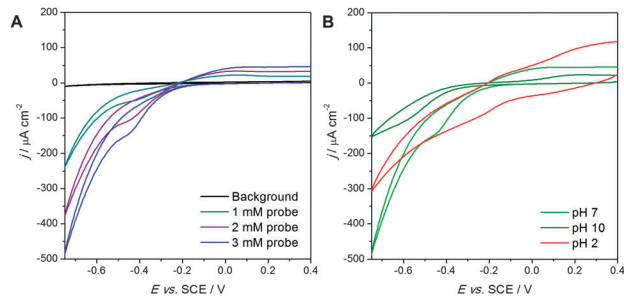


**Fig. 2** (A) Cyclic voltammograms obtained for ultrathick PMAA brushes examined at pH 7 in the absence (background) and the presence of increasing concentrations (1 mM, 2 mM and 3 mM) of ruthenium(III) hexamine. (B) Effect of pH on the CV of ultrathick PMAA brushes in the presence of a 3 mM redox probe. The pH values refer to those of the solutions used to condition the brushes.

concentration. This behavior would suggest that while for ultrathin brushes the electron transfer is dominated by tunneling, for the ultrathick ones the reduction of Ru(III) species inside the brushes proceeded *via* percolation between the redox centers after crossing the tunneling barrier.

The pH-responsive electrochemical behavior of ultrathick brushes was very similar to that reported for ultrathin PMAA brushes. The contribution of the capacitive currents was evident at pH 2 (Fig. 2b).

A further interesting feature of the electrochemistry of PMAA brushes on silicon wafer relates to the unusual crossing for the cyclic voltammograms for reduction and its scan reversal. For conventional electrochemical systems, curve crossing is interpreted as a consequence of a series of chemical reactions occurring within the electrochemical time scale of the voltammetry scan.<sup>48–52</sup> Due to the well-known stability and reliability of the hexamine ruthenium complex, however, this hypothesis would be hard to sustain in the present case. It is noteworthy to mention that until now there is only one example of this kind of behavior described for polymer brushes. In a recent paper,<sup>53</sup> E. Katz *et al.* observed curve crossing in the CV of poly(4-vinyl pyridine) brushes grafted from ITO in the presence of ferrocyanide as a redox probe and related it to the emergence of memimpedance (memory-impedance) properties.

**Electrochemical impedance spectroscopy (EIS).** From the results obtained by cyclic voltammetry it was apparent that PMAA brushes had a significant pH-controllable redox gating ability. This and other properties of both ultrathin and ultrathick brushes were investigated in more detail using electrochemical impedance spectroscopy (EIS).

When EIS was used to study the equilibration of the brushes with the supporting electrolyte, the data (complex plot and Bode plot, Fig. S4, ESI†) did not show any difference after 1 min and after 4 h of immersion, meaning that the brushes equilibrated very fast with the electrolyte. This may appear in contrast with the results obtained by ellipsometry, which required a longer time (~60 min) to achieve a stable thickness, *i.e.* to allow complete swelling of the brushes. However, spectroscopic ellipsometry is more sensitive than EIS to such small thickness changes. From an electrochemical point of view, EIS data show

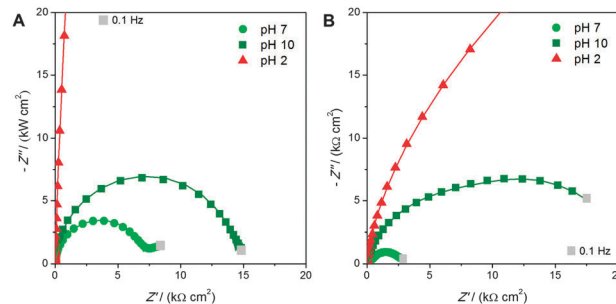
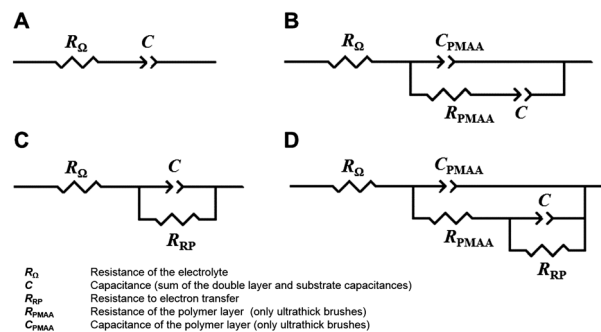


**Fig. 3** Complex plane plots obtained for (A) ultrathin and (B) ultrathick PMAA brushes as a function of pH in the presence of the redox probe. The pH values indicate the pH of the solutions used to condition the brushes.

that the equilibration of PMAA brushes with the supporting electrolyte occurs in a very short time (1 min). This is especially remarkable compared to the swelling behavior observed in our previous report for PHEMA and PAMA brushes, which required several hours to be completed.<sup>29</sup>

More insight on the pH-responsiveness of the brushes was then obtained by EIS in the absence and presence of ruthenium(III) hexamine. As for cyclic voltammetry, the brushes were first conditioned by immersion in solutions with different pH and impedance measurements were performed before and after the addition of the redox probe (3 mM). Complex plane plots in the presence of the redox probe are shown in Fig. 3, while the corresponding Bode plots are available in the ESI† (Fig. S5). Appropriate fitting of the plots with the equivalent electrical circuits (Scheme 2) allowed us to extract the characteristic electrochemical parameters of the brushes reported in Table 1 (ultrathin brushes) and Table 2 (ultrathick brushes).

In the absence of the redox probe, the ultrathin brushes showed in the complex plane plots a straight line with a slope  $> 45^\circ$  in all the range of frequencies and for all the pH values, replaced in the case of ultrathick brushes by a semicircle only at high frequencies (data not shown). The corresponding electrical equivalent circuits were composed by the electrolyte resistance  $R_\Omega$  in series with a capacitance  $C$  (representing the capacitance of the double layer and of the support) for ultrathin brushes (Scheme 2a) with the addition of PMAA capacitance  $C_{\text{PMAA}}$  and resistance  $R_{\text{PMAA}}$  in parallel for ultrathick brushes (Scheme 2b).



**Scheme 2** The equivalent circuits used to fit impedance data in the absence (A and B) and presence (C and D) of the redox probe for the ultrathin (A and C) and ultrathick (B and D) brush modified silicon electrodes.



**Table 1** The electrochemical parameters obtained by fitting the EIS data of ultrathin PMAA brushes in the presence of the redox probe

Sample (ultrathin brushes)	Potential [V]	$R_{\Omega}$ [ $\Omega$ cm <sup>2</sup> ]	$C$ [ $\mu$ F cm <sup>-2</sup> ]	$\alpha$	$R_{RP}$ [ $k\Omega$ cm <sup>2</sup> ]
pH 7 <sup>a</sup>	+0.25	26.63	4.39	0.99	—
	-0.15	26.95	3.53	0.99	—
	-0.25	26.96	3.38	0.99	—
pH 7	+0.25	24.40	4.54	0.98	1384
	-0.15	24.31	3.69	0.98	44
	-0.25	23.92	3.71	0.98	7
pH 10	+0.25	19.01	4.59	0.98	5089
	-0.15	19.13	3.63	0.98	95
	-0.25	18.98	3.57	0.98	14
pH 2	+0.25	19.21	4.42	0.98	21 579
	-0.15	19.68	3.42	0.98	18 224
	-0.25	19.75	3.26	0.98	14 252

<sup>a</sup> Without redox probe: background scan.**Table 2** The electrochemical parameters obtained by fitting the EIS data of ultrathick PMAA brushes in the presence of the redox probe

Sample (ultrathick brushes)	Potential [V]	$R_{\Omega}$ [ $\Omega$ cm <sup>2</sup> ]	$C_{PMAA}$ [ $\mu$ F cm <sup>-2</sup> ]	$\alpha_{PMAA}$	$R_{PMAA}$ [ $k\Omega$ cm <sup>2</sup> ]	$C$ [ $\mu$ F cm <sup>-2</sup> ]	$\alpha$	$R_{RP}$ [ $k\Omega$ cm <sup>2</sup> ]
pH 7 <sup>a</sup>	+0.25	20.00	14.50	0.87	19.78	16.93	0.69	—
	-0.15	20.23	11.29	0.88	18.16	15.40	0.67	—
	-0.25	20.00	10.88	0.87	18.67	15.24	0.73	—
pH 7	+0.25	24.40	4.54	0.91	15.11	28.37	0.62	—
	-0.15	24.31	3.69	0.91	12.27	30.17	0.64	7.31
	-0.25	23.92	3.71	0.92	10.67	42.58	0.89	1.96
pH 10	+0.25	18.45	18.10	0.88	19.56	34.85	0.71	—
	-0.15	18.01	13.99	0.87	17.83	43.47	0.87	28.50
	-0.25	18.64	13.33	0.87	12.84	77.41	0.92	7.74
pH 2	+0.25	17.30	6.75	0.93	24.49	12.57	0.50	—
	-0.15	17.61	5.03	0.94	24.33	10.61	0.50	225.50
	-0.25	17.33	4.83	0.94	27.32	4.83	0.59	130.59

<sup>a</sup> Without redox probe: background scan.

These last two elements appear only in the case of ultrathick brushes since for ultrathin ones the polymer film is not sufficiently thick to influence the electrochemical behavior of the electrode in the absence of the redox probe.

In the presence of the redox probe, the straight line becomes a semicircle for low frequencies, indicating the reaction of the redox probe for the two types of brushes (Fig. 3a and b). The electrical equivalent circuits show the addition of the electron transfer resistance  $R_{RP}$  in parallel with the capacitance  $C$  for both cases (Scheme 2c and d). It is noteworthy that the equivalent circuits used to model ultrathick brushes (Scheme 2b and d) are the same as reported previously for cationic brushes,<sup>29</sup> confirming the coherence of this new study. The trends of the complex plane plots are also confirmed by the Bode plots (ESI,† Fig. S4), in which one peak observed for ultrathin brushes and two peaks for ultrathick brushes correspond to the semicircles observed in the complex plots.

All the capacitances were modelled with a constant phase element CPE, reflecting the non-ideal homogeneity of the electrode surface defined as (eqn (1)):

$$CPE = [(C_{CPE}i\omega)^{\alpha}]^{-1} \quad (1)$$

where the parameter  $\alpha$  indicates the deviation from a purely capacitive behavior ( $\alpha = 1$ ) to a non-capacitive one ( $\alpha = 0.5$ ) and is thus an indicator of surface homogeneity.

Further important information can be obtained by examining the fitting parameters. First, the resistance of the supporting electrolyte  $R_{\Omega}$  remains the same for both types of brushes, as expected. In the absence of the redox probe, the capacitance  $C$  of ultrathin PMAA brushes is unaffected by pH, since the capacitance of the film is negligible and the  $\alpha$ -parameter values are very close to unity, confirming their high homogeneity and smooth surface already observed by AFM (Fig. S1, ESI†). On the other hand, for the ultrathick brushes, the relative contributions from the capacitance of the polymer brushes  $C_{PMAA}$  and the capacitance  $C$  can be easily differentiated. Moreover, these capacitances are strongly affected by pH with the following trend:  $C(\text{pH } 10) > C(\text{pH } 7) > C(\text{pH } 2)$ . This is in perfect accordance with the decrease of the overall charge, following the complete protonation of the carboxylic acid groups, and of the thickness, due to chain collapsing. The high values of the capacitances reported in Table 2 also explain the higher values of capacitive currents observed in the CV scans (Fig. 2), which hide the faradic peaks of the redox probe. The  $\alpha$ -parameter values are lower,



especially for the brushes at pH 2, compared to the ultrathin one suggesting a higher degree of disorder.

The resistance  $R_{\text{PMAA}}$  of the ultrathick brushes follows a trend which is specular to that of the capacitance:  $R_{\text{PMAA}}(\text{pH } 2) > R_{\text{PMAA}}(\text{pH } 7) > R_{\text{PMAA}}(\text{pH } 10)$ , reflecting the pH-dependency of the collapsed and swollen states of the brushes.

In the presence of the redox probe, the electron transfer resistance  $R_{\text{RP}}$  follows the same trend for both types of brushes  $R_{\text{RP}}(\text{pH } 2) > R_{\text{RP}}(\text{pH } 10) > R_{\text{RP}}(\text{pH } 7)$ , in accordance with the results obtained by cyclic voltammetry, confirming the best redox probe reaction for pH 7. Moreover, for ultrathick brushes it assumes lower absolute values in comparison with ultrathin ones due to the higher concentration of charge-carrier groups.

## Conclusions

Here, for the first time, PMAA brushes have been used as a pH-controlled and reversible ON/OFF switch to control the electrochemical properties of silicon wafers. Our findings significantly contribute to the understanding of silicon electrochemistry, considering that native oxide-coated silicon wafer is known to be a very poor electrode material. Moreover, surface-initiated polymerization, the approach by which PMAA brushes have been obtained, is compatible with state-of-the-art microfabrication procedures. These results open up completely new perspectives to develop polymer-Si electrochemical hybrid devices such as logic gates and sensors, in particular for microfluidics and lab-on-a-chip applications.

## Acknowledgements

Thanks are due to Ella Dehghani and Mohammad Divandari for assistance with ellipsometry. The authors gratefully acknowledge the financial support from the Swiss National Science Foundation (SNF).

## References

- U. Pischel, *Angew. Chem., Int. Ed.*, 2007, **46**, 4026.
- K. Szaciłowski, *Chem. Rev.*, 2008, **108**, 3481.
- G. de Ruiter and M. E. van der Boom, *Acc. Chem. Res.*, 2011, **44**, 563.
- C. A. Berven, M. N. Wybourne, L. Longstreth and J. E. Hutchison, *Physica E*, 2003, **19**, 246.
- V. R. de la Rosa, Z. Zhang, B. G. De Geest and R. Hoogenboom, *Adv. Funct. Mater.*, 2015, **17**, 2511.
- X. Wang, J. Zhou, T. Kin, E. Katz and M. Pita, *Bioelectrochemistry*, 2009, **77**, 69.
- M. Pita, S. Minko and E. Katz, *J. Mater. Sci.: Mater. Med.*, 2009, **20**, 457.
- E. Katz and S. Minko, *Chem. Commun.*, 2015, **51**, 3493.
- S. Mailloux, Y. V. Gerasimova, N. Guz, D. M. Kolpashchikov and E. Katz, *Angew. Chem., Int. Ed.*, 2015, **54**, 6562.
- P. Uhlmann, L. Ionov, N. Houbenov, M. Nitschke, K. Grundke, M. Motornov, S. Minko and M. Stamm, *Prog. Org. Coat.*, 2006, **55**, 168.
- R. Barbey, L. Lavanant, D. Paripovic, N. Schüwer, C. Sugnaux, S. Tugulu and H.-A. Klok, *Chem. Rev.*, 2009, **109**, 5437.
- G. Panzarasa, G. Soliveri, K. Sparnacci and S. Ardizzone, *Chem. Commun.*, 2015, **51**, 7313.
- G. Panzarasa, G. Soliveri, S. Ardizzone and K. Sparnacci, *Mater. Today*, 2015, **2**, 4183.
- G. Panzarasa, S. Aghion, G. Soliveri, G. Consolati and R. Ferragut, *Nanotechnology*, 2016, **27**, 02LT03.
- A. M. Jonas, K. Glinel, R. Oren, B. Nysten and W. T. S. Huck, *Macromolecules*, 2007, **40**, 4403.
- M. Dübner, N. D. Spencer and C. Padeste, *Langmuir*, 2014, **30**, 14971.
- G. J. Dunderdale and J. P. A. Fairclough, *Langmuir*, 2013, **29**, 3628.
- W. S. Choi, H. Y. Koo, J. Y. Kim and W. T. S. Huck, *Adv. Mater.*, 2008, **20**, 4504.
- O. Azzaroni, *J. Polym. Sci., Part A: Polym. Chem.*, 2012, **50**, 3225.
- X. Ma, Z. Xie, Z. Liu, X. Liu, T. Cao and Z. Zheng, *Adv. Funct. Mater.*, 2013, **23**, 3239.
- A. B. Rodríguez, M. R. Tomlinson, S. Khodabakhsh, J.-F. Chang, F. Cousin, D. Lott, H. Sirringhaus, W. T. S. Huck, A. M. Higgins and M. Geoghegan, *J. Mater. Chem. C*, 2013, **1**, 7736.
- Q. Li, Y. Zhang, H. Li, Q. Tang, L. Jiang, L. Chi, H. Fuchs and W. Hu, *Adv. Funct. Mater.*, 2009, **19**, 2987.
- J. C. Pinto, G. L. Whiting, S. Khodabakhsh, L. Torre, A. Rodríguez, R. M. Dalgliesh, A. M. Higgins, J. W. Andreasen, M. M. Nielsen, M. Geoghegan, W. T. S. Huck and H. Sirringhaus, *Adv. Funct. Mater.*, 2008, **18**, 36.
- B. Yu, H. Hu, D. Wang, W. T. S. Huck, F. Zhou and W. Liu, *J. Mater. Chem.*, 2009, **19**, 8129.
- T. K. Tam, M. Ornatska, M. Pita, S. Minko and E. Katz, *J. Phys. Chem. C*, 2008, **112**, 8438.
- Y. Wei, D. Gao, L. Li and S. Shang, *Polymer*, 2011, **52**, 1385.
- Y. Wang, M. Hung, C.-H. Lin, H. Lin and J. Lee, *Chem. Commun.*, 2011, **47**, 1249.
- K. Wolski, M. Szuwarzyński and S. Zapotoczny, *Chem. Sci.*, 2015, **6**, 1754.
- G. Panzarasa, G. Soliveri and V. Pifferi, *J. Mater. Chem. C*, 2016, **4**, 340.
- O. Azzaroni, A. A. Brown and W. T. S. Huck, *Adv. Mater.*, 2007, **19**, 151.
- S. Dai, P. Ravi and K. C. Tam, *Soft Matter*, 2008, **4**, 435.
- M. Zhang, P. Lin, M. Yang and F. Yan, *Biochim. Biophys. Acta, Gen. Subj.*, 2013, **1830**, 4402.
- M. Motornov, T. K. Tam, M. Pita, I. Tokarev, E. Katz and S. Minko, *Nanotechnology*, 2009, **20**, 434006.
- T. K. Tarn, M. Pita, M. Motornov, L. Tokarev, S. Minko and E. Katz, *Adv. Mater.*, 2010, **22**, 1863.
- Z. Li, H. Wang, X. Song, J. Yan, H. Hu and B. Yu, *J. Electroanal. Chem.*, 2014, **719**, 7.
- M. Privman, T. K. Tam, M. Pita and E. Katz, *J. Am. Chem. Soc.*, 2009, **131**, 1314.
- E. Katz, V. M. Fernández and M. Pita, *Electroanalysis*, 2015, **27**, 2063.



- 38 S. Xun, X. Song, L. Wang, M. E. Grass, Z. Liu, V. S. Battaglia and G. Liu, *J. Electrochem. Soc.*, 2011, **158**, A1260.
- 39 M. G. Santonicola, G. W. De Groot, M. Memesa, A. Meszynska and G. J. Vancso, *Langmuir*, 2010, **26**, 17513.
- 40 V. Bliznyuk, Y. Galabura, R. Burtovyy, P. Karagani, N. Lavrik and I. Luzinov, *Phys. Chem. Chem. Phys.*, 2014, **16**, 1977.
- 41 A. J. Parnell, S. J. Martin, C. C. Dang, M. Geoghegan, R. A. L. Jones, C. J. Crook, J. R. Howse and A. J. Ryan, *Polymer*, 2009, **50**, 1005.
- 42 H. Dong, H. Du and X. Qian, *J. Phys. Chem. B*, 2009, **113**, 12857.
- 43 R. F. Peetz, D. L. Dermody, J. G. Franchina, S. J. Jones, M. L. Bruening, D. E. Bergbreiter and R. M. Crooks, *Langmuir*, 1998, **14**, 4232.
- 44 Y. Gu, B. Akhremitchev, G. C. Walker and D. H. Waldeck, *J. Phys. Chem. B*, 1999, **103**, 5220.
- 45 Q. Li, S. Surthi, G. Mathur, S. Gowda, V. Misra, T. A. Sorenson, R. C. Tenent, W. G. Kuhr, S. I. Tamaru, J. S. Lindsey, Z. Liu and D. F. Bocian, *Appl. Phys. Lett.*, 2003, **83**, 198.
- 46 A. G. Scheuermann, K. W. Kemp, K. Tang, D. Q. Lu, P. F. Satterthwaite, T. Ito, C. E. D. Chidsey and P. C. Mc Intyre, *Energy Environ. Sci.*, 2016, **9**, 504.
- 47 N. Oyama, *J. Electrochem. Soc.*, 1980, **127**, 249.
- 48 C. Amatore, J. Pinson, J. M. Savéant and A. Thiebault, *J. Electroanal. Chem.*, 1980, **107**, 59.
- 49 J. M. Savéant, *Acc. Chem. Res.*, 1980, **13**, 323.
- 50 M. A. Fox and R. Akaba, *J. Am. Chem. Soc.*, 1983, **105**, 3460.
- 51 J. Heinze, A. Rasche, M. Pagels and B. Geschke, *J. Phys. Chem. B*, 2007, **111**, 989.
- 52 E. J. Lawrence, R. J. Blagg, D. L. Hughes, A. E. Ashley and G. G. Wildgoose, *Chem. – Eur. J.*, 2015, **21**, 900.
- 53 K. MacVittie and E. Katz, *J. Phys. Chem. C*, 2013, **117**, 24943.

